

# Driving Behavior Analysis and Traffic Improvement using Onboard Sensor Data and Geographic Information

Jun-Zhi Zhang and Huei-Yung Lin<sup>id</sup><sup>a</sup>

*Department of Electrical Engineering, National Chung Cheng University, Chiayi 621, Taiwan*

**Keywords:** Driving Behavior Analysis, Geographic Information System, Data Mining.

**Abstract:** In this paper, we present a method to extract the training and testing data from geographic information system (GIS) and global position system (GPS) for neural networks. Traffic signs, traffic lights and road information from the OpenStreetMap (OSM) and the government platform are compared with driving data and videos to extract images containing the important information. We also propose traffic improvement suggestions for intersections or roads by analyzing the relationship between driving behaviors, traffic lights, and road infrastructures. We use OBD-II and CAN bus logger to record more driving information, such as engine speed, vehicle speed, steering wheel steering angle, etc. We analyze the driving behavior using sparse automatic encoders and data exploration to detect abnormal and aggressive behavior. The relationship between the aggressive driving behavior and road facilities is derived by regression analysis, and some suggestions are provided for improving specific intersections or roads.

## 1 INTRODUCTION

In recent years, the field of self-driving cars has become more and more popular. Many companies and research institutes have started the development of autonomous vehicle systems. It is very likely to have self-driving cars and the vehicles controlled by human drivers co-exist on the road in the future. In this regard, one of the key components to the success of self-driving systems is to understand the human driving behavior in order to avoid the human-machine conflict (Dong and Lin, 2021). With the recent advances of machine learning techniques, the data-driven approaches have made the complicated human behavior modeling move a big step forward. Especially, some researches with significant progress have been conducted using deep learning (Hartford et al., 2016).

For the modern learning approaches, in addition to the design of network structures, another major issue is the requirement of a large amount of training data. In the automotive applications, this usually involves the data collection from on-board sensors and the information extraction for specific analysis purposes. These might include the images captured by the in-car cameras for environment perception, and the proprioceptive driving data recorded by the on-board diagnostics systems. In either case, it is necessary to

extract proper data segments for neural network training and testing. For instance, learning the road sign recognition uses certain traffic scene images, or modeling the driver's acceleration behavior uses selected gas pedal information. The use of large datasets for training is commonly agreed for deep neural networks to perform well or better.

In the early stage of related research, data annotation or labeling are mostly done manually, and sometimes through crowdsourcing such as using Amazon Mechanical Turk. For driving images, the dataset collected according to different tasks contains a variety of scenes and features. Since the selection and filtering of adequate data require significant time and human labor, it motivates a data management problem: How to search specific traffic scenes within a large amount of image sequences? In this work, we present a road scene extraction system for specific landmarks and indicators of the transportation infrastructure. The information derived from GIS (geographic information system) and GPS are used with the recorded driving videos to identify the road scenes with static objects such as traffic lights, traffic signs, bridge and tunnel, etc.

On the other hand, in addition to the exteroceptive sensors (such as LiDAR, GPS, camera, etc.), the information collected from proprioceptive sensors of the vehicle can also be used to analyze the driving behav-

<sup>a</sup><sup>id</sup> <https://orcid.org/0000-0002-6476-6625>

ior (Yeh et al., 2019). The sensor data derived directly from the vehicle operation can provide more comprehensive driving information. It allows the researchers and practitioners to study driving behaviors and traffic safety issues more precisely. In this paper, we adopt OBD-II (on-board diagnostics) and CAN bus (Controller Area Network) logger to collect data. By measuring a number of parameters at high sampling rate, it is possible to fully observe the driving behaviors in real life, and understand how they are affected by the traffic and road infrastructures.

To analyze the relationship between the driving behavior and the transportation infrastructure, its visualization on the map provides a way for better observation and investigation. We use machine learning-based methods to extract the unique features from the driving data and then map to the RGB color space to visualize the driving behavior. The data mining algorithms are adopted for data analysis and classify the driving behavior into four categories, from normal to aggressive. A regression analysis is then conducted on the relationship between the aggressive driving behavior and the road features of intersections.

## 2 RELATED WORK

### 2.1 Training and Testing Data Extraction

Due to the popularity of learning based algorithms in recent years, the acquisition of training and testing data has become an important problem. The current data extraction approaches are mainly divided into two categories, information-based and image-based extraction. Hornauer *et al.* and Wu *et al.* (Hornauer et al., 2019; Wu et al., 2018) proposed unsupervised image classification methods to extract to the images similarly to those provided by general users (Zhirong et al., 2018). In supervised classification, the data are labeled manually. People need to have similar understanding to annotate the same scene. Their network presents a concept based on feature similarity for first-person driving image query. However, it is not satisfactory for the requests of most users.

In addition to the image extraction and classification, Naito *et al.* developed a browsing and retrieval system for driving data analysis (Naito et al., 2010). The system provides a multi-data browser, a retrieval function based on query and similarity, and a quick browsing function to skip extra scenes. For the scene retrieval, the top  $N$  images highly similar to the currently driving scenario are retrieved from

the database. In this technique, while the image sequence is processed, the system calculates the similarity between the input scene and the scenes stored in the database. A pre-defined threshold is used to identify the similarity between the images. Since the method mainly searches the driving video itself, it is not able to know if the images contain the objects or information interested to the users for precise extraction.

### 2.2 Driving Behavior Analysis

In the past few years, the key technologies of automotive driving assistance systems have become more mature (Lin et al., 2020). However, the ‘autonomous’ vehicles are still not ready without the human drivers. Due to the current limitations of driving assistance systems, researchers and developers are seeking for the solutions to enhance the human driving capability. Since the driving habits are very difficult to change, it is expected to have a human-centered driving environment to avoid dangerous situations. By understanding the relationship among the traffic lights, road infrastructure and driving behavior, some transportation improvement suggestions can be provided. Besides, knowing the human reaction is also a crucial issue in the future world with mixed human drivers and self-driving cars.

For driving behavior analysis, Liu *et al.* proposed a method using various types of sensors connected to the control area network (Liu et al., 2014; Liu et al., 2017). A deep sparse autoencoder is then used to extract the hidden features from driving data to visualize the driving behavior. Alternatively, Constantinescu *et al.* used both PCA and HCA methods to analyze the driving data (Constantinescu et al., 2010). The performance of the algorithms is verified by classifying the driving behavior into six categories according to different aggressiveness. In the study of Kharrazi *et al.*, the driving behavior is classified into three categories, calm, normal and aggressive, by a method using quartile and Kmeans (Kharrazi et al., 2019). The analysis has demonstrated that Kmeans is able to provide good driving behavior classification results.

In the above methods, the correlation between the driving behavior and the environment is not investigated. For the discussion of more specific events, Tay *et al.* used the regression model to associate driving accidents with the environment (Tay et al., 2008). Wong *et al.* used a negative binomial regression to analyze the number of driving accidents and the road features of the intersection (Wong, 2019). It can help us understand the relationship between the accidents and road features. The road intersection can also be

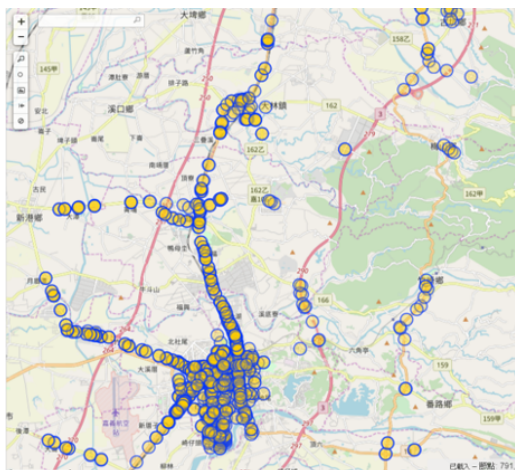


Figure 1: The traffic light information shown on the OpenStreetMap. The yellow dots indicate the locations of traffic lights on main roads.

improved by the simulation carried out based on the analysis results. Schorr *et al.* recorded the driving data in one and two-way lanes (Schorr *et al.*, 2016). Based on ANOVA analysis, the conclusion about the impact of the lane width to the driving behavior is drawn. Mohammad *et al.* investigated how the accidents were affected specific driving behaviors through a number of questionnaires and interviews (Abojadah *et al.*, 2014). They used regression analysis to derive the correlation between the number of accidents and the types of dangerous driving behaviors.

Regarding the improvement on transportation infrastructures, various suggestions were proposed for different designs of roads and intersections. Chunhui *et al.* proposed to optimize the signal lights at the intersections to make the pedestrian crossing easier (Chunhui *et al.*, 2017; Wang *et al.*, 2019). The efficiency of intersections is improved by reducing the conflicts between the turning vehicles and pedestrians. Ma *et al.* proposed to add a dedicated left-turn lane and left turn waiting area according to the average daily traffic volume at the intersection (Ma *et al.*, 2017). The proposed method is able to accommodate more vehicles waiting for left turn. They also analyze three common left-turn operation scenarios at the intersections and compare their differences. In addition to the suggestions for road infrastructures, there also exist some improvements based on the traffic light analysis. In the recent work, Anjana *et al.* presented a method based on different traffic volumes at the intersections to evaluate the safety caused by the green time of the traffic light (Anjana and Anjaneyulu, 2015).

### 3 DATASET EXTRACTION

We first collect traffic lights, traffic signs and road information on the OpenStreetMap (OSM) and the government's GIS-T transportation geographic information storage platform of the as the locations of interest for image data extraction. Figure 1 illustrates an example of the traffic light information shown on the OSM. The yellow dots indicate the locations of traffic lights on main roads. For image data extraction, the transportation infrastructure and road information are used to identify the locations of interest using the GPS coordinates. We compare the GPS information of the driving data and the locations of interest. The associated images are then extracted and stored in video sequences for specific application uses (such as the training and testing data for traffic light detection).

The specifications of the driving recorder contain the images with the resolution of  $1280 \times 720$  and  $110^\circ$  FOV (field-of-view) in the horizontal direction. To extract the suitable image data, the users need to consider a geographic range of the interested target. As a typical example of road scene extraction with traffic lights, the size of the traffic signal in the image might be larger than  $25 \times 25$  pixels for specific tasks. This corresponds to about 50 meters away from the vehicle, so the video should be pushed back 5 seconds to start the image extraction.

A program interface is created for users to easily operate the data and assign the parameters. As shown in Figure 2, it consists of folder selection, item menu for extraction, OSM map display and driving image screen. The user first select the folder where the driving record video and driving GPS information are located, and the folder where the extracted image will be stored, followed by the selection of the traffic infrastructure or road information to be extracted. On the interface, the vehicle's GPS trajectory and the user selected traffic infrastructures simultaneously overlay on the OSM window, and the synchronized driving video is displayed on the right for inspection.

### 4 DRIVING BEHAVIOR ANALYSIS

In this paper, we mainly focus on the analysis of driving behavior and the correlation with traffic and road features. The common relationship is first established and the studies on specific scenarios are then carried out. The driving behavior is classified into normal and aggressive, and analyzed through data visualization and the regression model on the number of aggressive driving behaviors and road features.

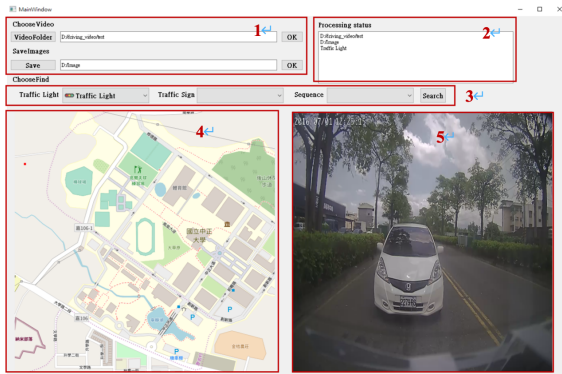


Figure 2: The user interface for image data extraction. 1. folder selection, 2. processing status display, 3. extraction item menu, 4. driving trajectory display, and 5. driving video display.

#### 4.1 Data Collection

The tools for data collection in this work include ODB-II (Malekian et al., 2014) and CANbus loggers. Unlike most previous work which only use the information obtained from GPS receivers (with GPS messages, vehicle speed and acceleration), OBD-II and CANbus loggers are able to collect various types of driving data to analyze in more details. The specific data types used for our driving behavior analysis are as follows:

- OBD-II: engine rotating speed, engine load, throttle pedal position, acceleration XYZ, and vehicle speed.
- CANbus logger: engine rotating speed, throttle pedal position, braking pedal position, steering angle, wheel speed, and vehicle speed.
- GPS receiver: GPS and UTC.

In addition, we also use two public datasets, DDD17 dataset (Binas et al., 2017) and UAH Drive-set (Romera et al., 2016). The datasets are acquired by the driving monitoring application, DriveSafe, and mainly used to verify the classification and analysis methods (Bergasa et al., 2014).

#### 4.2 Visualization of Driving Behavior

The relationship between the driving behavior and traffic infrastructures can be observed by the data visualization on the map. We use the sparse autoencoder (SAE) to extract features from the driving data, compress the high-dimensional features into three dimensions, and mapping to RGB space for display on the OpenStreetMap (Liu et al., 2017). The loss func-

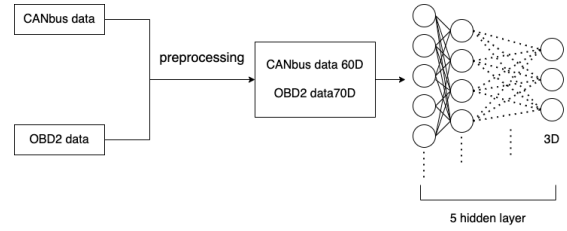


Figure 3: The flowchart and network structure for driving behavior analysis.

tion with sparse constraints is given by

$$J_{sparse}(W, b) = J(W, b) + \beta \sum_{j=1}^{s_2} KL(\rho \parallel \hat{\rho}_j) \quad (1)$$

The difference between SAE and autoencoder (AE) is that a penalty term is added to the loss function, so the activation of the hidden nodes drops to the value we need. Using this property, the relative entropy is added to the loss function to penalize the value of the average activation degree far away from the level  $\rho$ . The parameters can keep the average activation degree of hidden nodes at the level. Thus, the loss function only needs to add the penalty term of relative entropy without sparse constraints.

Figure 3 illustrates the structure to visualize the driving behavior. The network contains 9 hidden layers, and the dimensionality reduction of each layer is half the number of nodes in the previous layer. Our data collected by OBD-II contain 7 types, and become 70 dimensions after windowing process. Thus, the dimension reduction in the network is  $70 \rightarrow 35 \rightarrow 17 \rightarrow 8 \rightarrow 3 \rightarrow 8 \rightarrow 17 \rightarrow 35 \rightarrow 70$ , and the features are extracted by the last 5 layers. The data collected by CANbus logger contain 6 types, and are processed to 60 dimensions after windowing. Likewise, the input to the network consists of 60 nodes, and the dimension reduction is given by  $60 \rightarrow 30 \rightarrow 15 \rightarrow 7 \rightarrow 3 \rightarrow 7 \rightarrow 15 \rightarrow 30 \rightarrow 60$ . Finally, the driving behavior is visualized on the OpenStreetMap.

We use the Kmeans clustering algorithm to further classify the driving behavior. The elbow method is used to find the most appropriate  $k$  value to classify the driving behavior according to different aggressiveness (Thorndike, 1953). From normal to aggressive, it is classified into four levels, and the most aggressive driving behavior is marked on the OSM.

#### 4.3 Negative Binomial Regression

We refer to (Wong, 2019) and use negative binomial regression model to analyze the road features at intersections and interchanges. It is an extended version of Poisson regression to deal with the data overdispersed problem. The negative binomial regression



model

$$\mu_i = \exp(\beta_1 x_{1i} + \beta_2 x_{2i} + \dots + \beta_k x_{ki} + \varepsilon_i) \quad (2)$$

is used to predict the number of aggressive driving behavior  $\mu_i$ , where  $\beta$  is the correlation term associated with each road feature parameter, and  $\varepsilon_i$  is an error term. Next, we need to verify if the data are over-dispersed, so Pearson's chi-squared test is carried out (Pearson, 1900). When the ratio is greater than 1, the data is considered to be over-dispersed.

To evaluate whether the Poisson regression or negative binomial regression can better fit our data, Akaike information criterion (AIC) is calculated for these two models (Akaike, 1974). AIC is an effectiveness measure of data fitting on regression models given by

$$AIC = 2k - 2\ln(L) \quad (3)$$

where  $k$  is the number of features and  $\ln(L)$  is the maximum likelihood. A smaller AIC value implies a better fitting model. As an example case, the maximum likelihoods of Poisson and negative binomial regression are -21.457 and -21.758 respectively, and the AIC values are 58.914 and 59.516 respectively. It shows that the negative binomial regression model has a smaller AIC. Thus, it is used as the model for our analysis.

After classifying the driving behavior by Kmeans, it is found that the aggressive driving behavior occurs more frequently at the interchanges and intersections. The negative binomial regression analysis is carried out on these two specific driving scenarios. We adopt the road features proposed by Wong (Wong, 2019) and those commonly appeared in Taiwan road scenes as follows.

1. Interchange: (1) section length, (2) lane width, (3) speed limit, (4) traffic flow.
2. 4-Arm Intersection: (1) without lane marking, (2) straight lane marking, (3) left lane marking, (4) right lane marking, (5) shared lane marking, (6) shared lane marking at roadside, (7) motorcycle priority, (8) branch road.
3. 3-Arm Intersection: (1) without lane marking, (2) straight lane marking, (3) shared lane marking at roadside, (4) lane ratio, (5) motorcycle priority, (6) branch road.

## 5 EXPERIMENTS

The experiments contain two parts: One is the system for the extraction of training and testing dataset, and the other is the driving behavior analysis based on the driving and road features.

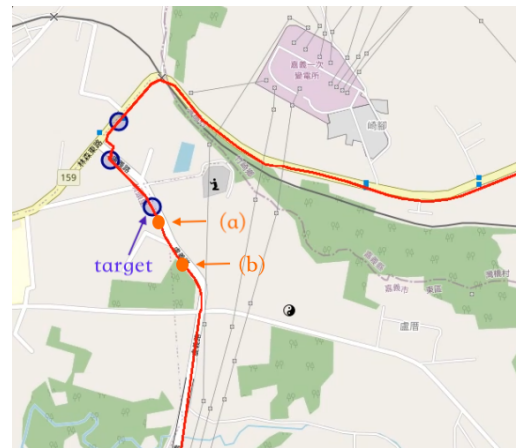


Figure 4: The driving trajectory (marked in red curve) and traffic light positions (marked in purple circles) displayed on the OpenStreetMap. The orange dots (a) and (b) correspond to the images shown in Figures 5(a) and 5(b), respectively.



(a) Long range image. (b) Short range image.

Figure 5: The images containing traffic lights extracted from the map in 4, corresponding to the locations (a) and (b), respectively.

### 5.1 Extraction of Training and Testing Data

In this experiment, we demonstrate the image data extraction for the road scenes with traffic lights. Figure 4 shows the driving trajectory (marked in red curve) and traffic light positions (marked in purple circles) displayed on OSM. The driving video is filtered through the extraction system to contain the traffic lights from the far to near distance. The extracted images as shown in Figures 5(a) and 5(b) correspond to the orange dots (a) and (b) on the map (in Figure 4), respectively.

### 5.2 Driving Behavior Analysis

For driving behavior analysis, the visualization and Kmeans classification are presented first, followed by the analysis on the driving behavior and road features.



Figure 6: The visualized driving behavior. The aggressive driving data and traffic lights are marked on the OpenStreetMap. The red circle location corresponds to the data enclosed by red in Figure 7 and the driving image shown in Figure 8.

### 5.2.1 Visualization and Kmeans Classification

In this experiment, whether Kmeans can effectively classify the driving behavior is verified first. We use five segments of driving data in UAH Drive-set, and the drivers are in normal and aggressive behaviors separately. In each data segment, 50 samples are taken for classification. The results are shown in Table 1 with the percentage of correct classification, where D1 – D5 represent five drivers. N and A are the normal and aggressive driving, respectively. The table illustrates that Kmeans is able to provide satisfactory classification results on normal and aggressive driving behaviors.

Figure 6 shows the driving behavior (including aggressive driving) using the driving data collected by ourselves visualized on OpenStreetMap with the traffic light location information. The driving data chart and the image acquired by a car digital video recorder are shown in Figures 7 and 8, respectively. By observing the information from these three aspects, the correlation among them can be analyzed. In this example, the aggressive driving behavior at location indicated by the red circle (Figure 6) is caused by a pedestrian passing through the intersection (Figure 8), which leads to the braking and turning of the vehicle (Figure 7).

By visualizing the driving behavior and displaying the aggressive driving behaviors on OSM with reference to the driving video, we are able to observe the correlation between the driving behavior and traffic infrastructure. Three situations are analyzed as follows.

- a. The influence of two-way lanes on the driving behavior: We found that the vehicle speed in a two-way lane is higher than a one-way lane. Thus,

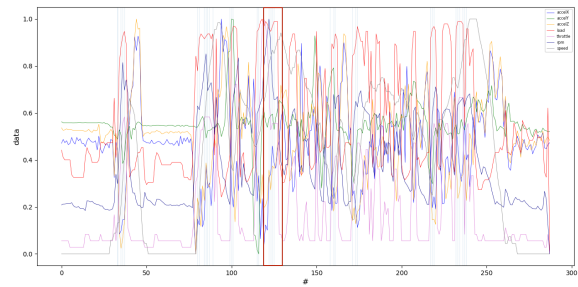


Figure 7: The driving data chart. The red frame corresponds to the location indicated by the red circle in Figure 6 and the driving image in Figure 8.



Figure 8: The image acquired at the location corresponding to the circle in Figure 6. A pedestrian passing through the intersection leads the braking of the vehicle as illustrated in Figure 7.

the aggressive driving behaviors with fast driving and emergency braking are more likely to occur in two-way lanes.

- b. The influence of traffic lights on the driving behavior: We found that most of the aggressive driving behaviors occurred at intersections. There might be many reasons, such as fast changing signals and the poor design of the road. These generally cause more conflicts between the drivers and other vehicles.
- c. The influence of interchanges on the driving behavior: In the highway traffic, we found that most of the aggressive driving behaviors occur at interchanges. A vehicle entering the entrance of the interchange tends to drive into the inner lane. This generally causes the other drivers to change lanes or slow down.

### 5.2.2 Negative Binomial Regression

Since the aggressive driving behaviors frequently occur near the intersections and interchanges, we further investigate these driving scenarios using negative binomial regression analysis on the correlation between the number of aggressive behaviors and road features.

Table 1: The Kmeans classification performance on UAH Drive-set.

D1		D2		D3		D4		D5	
N	A	N	A	N	A	N	A	N	A
100%	80%	100%	100%	100%	96%	98%	100%	98%	98%

```

Generalized Linear Model Regression Results
-----
Dep. Variable:          AGGRE      No. Observations:      21
Model:                 GLM         Df Residuals:          13
Model Family:          NegativeBinomial  Df Model:              7
Link Function:         log         Scale:                 1.0000
Method:                IRLS        Log-Likelihood:        -43.927
Date:                  Sat, 02 May 2020    Deviance:              1.1128
Time:                  07:55:51      Pearson chi2:          1.12
No. Iterations:        5
Covariance Type:      nonrobust
-----
                    coef    std err          z      P>|z|      [0.025   0.975]
-----
Intercept          1.9725    0.367          5.379    0.000        1.254    2.691
LEFT              -0.0342    0.099         -0.344    0.731       -0.229    0.160
STRA               0.0521    0.020          2.632    0.008        0.013    0.091
RIGHT             -0.0156    0.279         -0.056    0.955       -0.562    0.531
TWO               0.0114    0.102          0.111    0.912       -0.189    0.212
SHARE             -0.1328    0.062         -2.130    0.033       -0.255    -0.011
NO                0.0521    0.020          2.632    0.008        0.013    0.091
MOTOR             0.0826    0.197          0.419    0.675       -0.304    0.469
CROSS             -0.1153    0.144         -0.802    0.423       -0.397    0.167
-----

```

(a) The regression result at a 4-arms intersection.

```

Generalized Linear Model Regression Results
-----
Dep. Variable:          AGGRE      No. Observations:      20
Model:                 GLM         Df Residuals:          15
Model Family:          NegativeBinomial  Df Model:              4
Link Function:         log         Scale:                 1.0000
Method:                IRLS        Log-Likelihood:        -68.375
Date:                  Mon, 20 Apr 2020    Deviance:              37.665
Time:                  06:47:29      Pearson chi2:          33.2
No. Iterations:        7
Covariance Type:      nonrobust
-----
                    coef    std err          z      P>|z|      [0.025   0.975]
-----
Intercept          2.6926    1.375          1.958    0.050       -0.003    5.388
LONG              -0.0006    0.000         -4.018    0.000       -0.001    -0.000
LANE              -0.6021    0.313         -1.923    0.054       -1.216    0.012
LIMIT            0.0711    0.011          6.292    0.000        0.049    0.093
FLOW             -5.887e-06  1.51e-05       -0.390    0.696       -3.54e-05  2.37e-05
-----

```

(b) The regression result at a highway interchange.

Figure 9: The negative binomial regression analysis results for a 4-arm intersection and a highway interchange. (a) Intercept: the error term of regression model, LEFT: left turn lane mark, STRA: straight lane mark, RIGHT: right turn lane mark, TWO: shared lane mark, SHARE: shared lane mark on the side of the road, NO: no lane mark, MOTOR: the number of priority locomotive lanes, CROSS: the number of branch roads and the coefficient term is the parameter by the regression model. (b) LONG: the length of interchange, LANE: the width of the lane, LIMIT: the ramp speed limit, and FLOW: the average daily traffic volume.

The P-value is used to evaluate whether the feature has a significant impact on aggressive driving behavior (Dahiru, 2008). Two driving scenarios are examined as follows.

**4-Arms Intersection:** There are eight different road features at the intersections as defined previously. After the regression analysis as shown in Figure9(a), we see the features that have great impacts on the aggressive driving behaviors include ‘straight lane marking’, ‘shared lane marking at roadside’ and ‘without lane marking’. The influences of these features on the driving behaviors are positive correlation, negative correlation and

positive correlation, respectively. When “ $P > |z|$ ”  $< 0.05$ , the feature is important affects the aggressive behavior.

**Highway Interchange:** There are four different road features defined for the highway. After the regression analysis as shown in Figure 9(b), we see the features that have great impacts on the aggressive driving behaviors are ‘speed limit’ and ‘length of interchange’. The influences of these features on the driving behaviors are positive correlation and negative correlation, respectively.

## 6 CONCLUSIONS

This paper presents the image data extraction based on geographic information and driving behavior analysis using various types of driving data. The traffic infrastructure and GPS information are used to extract specific road scenes for network training and testing purposes. We use OBD-II and CANbus loggers to acquire driving data, and classify the driving behaviors using SAE feature extraction and Kmeans algorithm. The negative binomial regression analysis is performed for specific scenarios. Our result show that lane ratios, without lane markings, and straight lane markings are important features which affect the aggressive driving behavior. In the end, we present the traffic improvements based on the analysis for a case study at an intersection.

## ACKNOWLEDGMENTS

This work was financially/partially supported by Create Electronic Optical Co., LTD, Taiwan.

## REFERENCES

Abojaradeh, M., Jrew, B., and Al-Ababsah, H. (2014). The effect of driver behavior mistakes on traffic safety. *Journal of Civil and Environment Research*, 6:39–54.

Akaike, H. (1974). A new look at the statistical model identification. *IEEE Transactions on Automatic Control*, 19:716—723.

- Anjana, S. and Anjaneyulu, M. (2015). Safety analysis of urban signalized intersections under mixed traffic. *Journal of Safety Research*, 52:9–14.
- Bergasa, L. M., Almería, D., Almazán, J., Yebes, J. J., and Arroyo, R. (2014). Drivesafe: an app for alerting inattentive drivers and scoring driving behaviors. *IEEE Intelligent Vehicles Symposium(IV)*, pages 240–245.
- Binas, J., Neil, D., Liu, S.-C., and Delbruck, T. (2017). Ddd17: End-to-end davis driving dataset. *Workshop on Machine Learning for Autonomous Vehicles*, pages 1–9.
- Chunhui, Y., Wanjing, M., Ke, H., and Xiaoguang, Y. (2017). Optimization of vehicle and pedestrian signals at isolated intersections. *Transportation Research Part B: Methodological*, 98(C):135–153.
- Constantinescu, Z., Marinoiu, C., and Vladoiu, M. (2010). Driving style analysis using data mining techniques. *International Journal of Computers and Communications and Control*, 5(5):654–663.
- Dahiru, T. (2008). P-value, a true test of statistical significance? a cautionary note. *Annals of Ibadan Postgraduate Medicine*, 6:21–26.
- Dong, B. T. and Lin, H. Y. (2021). An on-board monitoring system for driving fatigue and distraction detection. In *2021 IEEE International Conference on Industrial Technology*, Valencia, Spain. (ICIT 2021).
- Hartford, J. S., Wright, J. R., and Leyton-Brown, K. (2016). Deep learning for predicting human strategic behavior. In Lee, D. D., Sugiyama, M., Luxburg, U. V., Guyon, I., and Garnett, R., editors, *Advances in Neural Information Processing Systems 29*, pages 2424–2432. Curran Associates, Inc.
- Hornauer, S., Yellapragada, B., Ranjbar, A., and Yu, S. (2019). Driving scene retrieval by example from large-scale data. In *Proceedings of the IEEE/CVF Conference on Computer Vision and Pattern Recognition (CVPR) Workshops*.
- Kharrazi, S., Frisk, E., and Nielsen, L. (2019). Driving behavior categorization and models for generation of mission-based driving cycles. *IEEE Intelligent Transportation Systems Conference*, pages 1349–1354.
- Lin, H. Y., Dai, J. M., Wu, L. T., and Chen, L. Q. (2020). A vision based driver assistance system with forward collision and overtaking detection. *Sensors*, 20(18):100–109.
- Liu, H., Taniguchi, T., Takano, T., Tanaka, Y., Takenaka, K., and Bando, T. (2014). Visualization of driving behavior using deep sparse autoencoder. pages 1427–1434.
- Liu, H., Taniguchi, T., Tanaka, Y., Takenaka, K., and Bando, T. (2017). Visualization of driving behavior based on hidden feature extraction by using deep learning. *IEEE Transactions on Intelligent Transportation Systems*, 18(9):2477–2489.
- Ma, W., Liu, Y., jing Zhao, and Wu, N. (2017). Increasing the capacity of signalized intersections with left-turn waiting areas. *Transportation Research Part A: Policy and Practice*, 105:181–196.
- Malekian, R., Moloisane, N. R., Nair, L., Maharaj, B., and Chude-Okonkwo, U. A. (2014). Design and implementation of a wireless obd ii fleet management system. *IEEE Sensors Journal*, 13:1154–1164.
- Naito, M., Miyajima, C., Nishino, T., Kitaoka, N., and Takeda, K. (2010). A browsing and retrieval system for driving data. *IEEE Intelligent Vehicles Symposium*, pages 1159–1165.
- Pearson, K. (1900). X. on the criterion that a given system of deviations from the probable in the case of a correlated system of variables is such that it can be reasonably supposed to have arisen from random sampling. *The London, Edinburgh and Dublin Philosophical Magazine and Journal of Science*, pages 157–175.
- Romera, E., Bergasa, L. M., and Arroyo, R. (2016). Need data for driver behaviour analysis? presenting the public uah-driveset. *International Conference on Intelligent Transportation Systems (ITSC)*, pages 387–392.
- Schorr, J., Hamdar, S. H., and Silverstein, C. (2016). Measuring the safety impact of road infrastructure systems on driver behavior: Vehicle instrumentation and exploratory analysis. *Journal of Intelligent Transportation Systems*.
- Tay, Richard, Rifaat, Shakil, Chin, and Hoong (2008). A logistic model of the effects of roadway, environmental, vehicle, crash and driver characteristics on hit-and-run crashes. *Accident; analysis and prevention*, 40:1330–6.
- Thorndike, R. L. (1953). Who belongs in the family? *Psychometrika*, 18(4):267–276.
- Wang, Y., Qian, C., Liu, D., and Hua, J. (2019). Research on pedestrian traffic safety improvement methods at typical intersection. *2019 4th International Conference on Electromechanical Control Technology and Transportation (ICECTT)*, pages 190–193.
- Wong, C. K. (2019). Designs for safer signal-controlled intersections by statistical analysis of accident data at accident blacksites. *IEEE Access*, 7:111302–111314.
- Wu, Z., Xiong, Y., Yu, S. X., and Lin, D. (2018). Unsupervised feature learning via non-parametric instance discrimination. *2018 IEEE/CVF Conference on Computer Vision and Pattern Recognition*, pages 3733–3742.
- Yeh, T. W., Lin, S. Y., Lin, H. Y., Chan, S. W., Lin, C. T., and Lin, Y. Y. (2019). Traffic light detection using convolutional neural networks and lidar data. In *2019 International Symposium on Intelligent Signal Processing and Communication Systems (ISPACS)*, pages 1–2.
- Zhirong, W., A, E. A., and Stella, Y. (2018). Improving generalization via scalable neighborhood component analysis. *European Conference on Computer Vision (ECCV) 2018*.